DALTON
FULL PAPER

Structure, spectroscopy and electrochemistry of the bis(2,2′-bipyridine)(salicylato)ruthenium(II) complex

Vera R. L. Constantino,* Henrique E. Toma, Luiz F. C. de Oliveira, Francisca N. Rein, Reginaldo C. Rocha and Denise de Oliveira Silva

Instituto de Química, Universidade de São Paulo, Caixa Postal 26077, CEP 05599-970, São Paulo, SP, Brazil

Received 1st September 1998, Accepted 16th March 1999

The bis(2,2′-bipyridine)(salicylato)ruthenium(II) complex has been prepared and characterized by means of single crystal X-ray diffraction, electrochemistry and resonance Raman spectroscopy. The electronic bands in the visible region have been assigned to Ru–bipy charge-transfer transitions and discussed in terms of ZINDO/S semiempirical calculations. Spectroelectrochemical measurements have been performed in order to elucidate the nature of the electrochemical waves in the cyclic voltammograms. The green complex generated by oxidation of the complex at 0.25 V has been isolated, revealing substantial ruthenium–salicylate electronic mixing, as deduced from the corresponding resonance Raman spectra. Further oxidations at 1.2 and 1.4 V have been observed and ascribed to hydroxylation of the salicylate semiquinone ligand in the complex.

Introduction

Salicylic acid is a typical bidentate ligand for transition metal ions. In addition to a wide range of biological applications, it is also a commonly used radical scavenger, reacting rapidly with hydroxyl radicals and singlet oxygen species.[1] The presence of the carboxy-phenolic group supports a number of analytical applications, as exemplified by the colorimetric detection of iron(III) species. In spite of its traditional use in co-ordination chemistry, to our knowledge, the expected similarities with the redox active, non-innocent quinonoid ligands[2–6] have never been exploited up to the present time. A strong covalence involving this type of ligands has been suggested for the corresponding ruthenium–polypyridine complexes, giving rise to a very interesting discussion concerning the assignment of the redox states and valence localization.[2–6] Along this line, here we report a detailed investigation on the spectroscopic and electrochemical behavior of the bis(2,2′-bipyridine)(salicylato)-ruthenium(II) complex.

Experimental and computation

Preparation

Bis(2,2′-bipyridine)(salicylato)ruthenium(II) tetrahydrate. The complex $[Ru(bipy)_2(sal)]\cdot 4H_2O$ (bipy = 2,2′-bipyridine, sal = salicylate ion) was synthesized by treating 1 mmol of $[Ru(bipy)_2Cl_2]$[7] with 1.3 mmol of salicylic acid (Aldrich) and 4 mmol of NaOH, in a 2:1 water–ethanol mixture (140 cm^3), under reflux for 15 h, in the presence of an argon atmosphere. The reaction mixture was kept in a refrigerator for about five days until precipitation of the complex. The solid was collected on a filter and washed with a small amount of cold water and acetone (Found: C, 53.4; H, 4.5; N, 9.3. $C_{27}H_{28}N_4O_7Ru$ requires C, 52.2; H, 4.5; N, 9.0%). The water content was determined thermogravimetrically as 10.9% of weight, corresponding to four water molecules per mol of ruthenium. Yield: 67%.

Bis(2,2′-bipyridine)(salicylato)ruthenium(III) hexafluorophosphate dihydrate. The complex $[Ru(bipy)_2(sal)]PF_6\cdot 2H_2O$ was obtained by treating equimolar amounts of $[Ru(bipy)_2(sal)]\cdot 4H_2O$ and $AgNO_3$ in 10 cm^3 of 1:1 water–ethanol (v/v) solution. After 15 min the green solution was filtered and the solvent removed in a rotary evaporator. The residue was dissolved with a small amount of water and a green solid precipitated by adding NH_4PF_6. The product was collected on a filter, washed with small amounts of cold water and diethyl ether, and dried under vacuum (Found: C, 44.1; H, 3.2; N, 7.6. $C_{27}H_{24}F_6N_4O_5PRu$ requires C, 44.4; H, 3.3; N, 7.6%). Yield: 80%.

Crystal structure determination of $[Ru(bipy)_2(sal)]\cdot 4H_2O$

Single crystals of $[Ru(bipy)_2(sal)]\cdot 4H_2O$ were obtained from a water–ethanol reaction mixture by cooling at refrigerator temperature and a purple crystal of dimensions 0.40 × 0.30 × 0.20 mm was mounted on the top of a glass fiber. Intensity data were collected on an Enraf-Nonius MACH-3S diffractometer using the CAD4-EXPRESS software.[8] The measurements were carried out at room temperature using graphite monochromated Mo-Kα ($\lambda = 0.71069$ Å) radiation. The data were corrected for absorption using the MOLEN software package.[9] The positions of the metal atom were located by the Patterson method in SHELXS 86[10] and the positions of the other non-hydrogen atoms through a sequence of Fourier-difference maps and least-squares cycles. The refinement by full-matrix least-square procedures was carried out by standard methods with the use of SHELXL 93.[11] No hydrogen atoms were placed on the water oxygen atoms except for O(4).

Crystal data. $C_{27}H_{28}N_4O_7Ru$, $M = 621.60$, monoclinic, space group $P2_1/n$ (no. 14), $a = 9.888(3)$, $b = 16.899$ (2), $c = 15.560$ (2) Å, $\beta = 90.90$ (2) °, $V = 2599.7(9)$ Å^3, $T = 293$ K, $Z = 4$, μ(Mo-Kα) = 0.658 mm^{-1}, 4840 reflections collected, 4560 unique ($R_{int} = 0.1372$). $R1 = 0.0582$, $wR2 = 0.1417$ for $I > 2\sigma(I)$; R_1, $wR2 = 0.1055$, 0.1733 (all data); goodness of fit (on F^2) = 1.049.

CCDC reference number 186/1395.

Physical techniques

The electronic spectra of the complexes were recorded on a Hewlett-Packard model 8452-A diode-array spectrophotometer or on a Guided-Wave model 260 fiber-optics instrument. Cyclic voltammetry measurements were carried out with a Princeton Applied Research instrument consisting of a model 173 potentiostat and a model 175 universal programmer. A platinum electrode was employed for the measurements using a

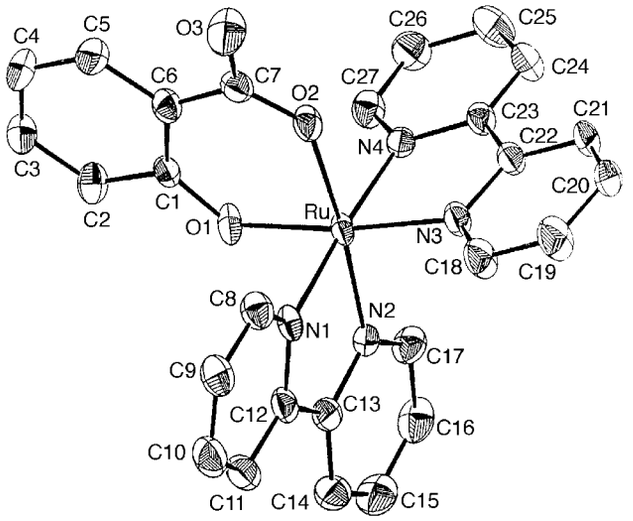

Fig. 1 An ORTEP[20] drawing of the molecular structure and atom numbering scheme for [Ru(bipy)$_2$(sal)]. The atoms are represented by thermal ellipsoids at 40% probability level.

Luggin capillary with Ag–$AgNO_3$ (0.010 M) reference electrode ($E°$ = 0.503 V *versus* NHE)[12] in dmf containing 0.10 M Et_4NClO_4. A platinum wire was used as the auxiliary electrode. The spectroelectrochemical measurements were carried out as previously described.[13] The Raman spectra were obtained as reported previously using Jarrell-Ash[14,15] or Renishaw[16] equipment, EPR spectra for the [Ru(bipy)$_2$(sal)]PF_6 solid complex on a Bruker EMX spectrometer, at room temperature and 220 K (working conditions: 2000–4000 G, 9.312 GHz microwave power = 20 mW, modulation frequency = 100 kHz, mod. amplitude 12 G). Thermogravimetric measurements were carried out using a Shimadzu model TGA-50 instrument.

Molecular calculations

Semiempirical molecular orbital calculations were carried out by using the INDO/S method[17] within the ZINDO[18] program from Molecular Simulation Inc., using default energy parameters but with β(4d) = −16 eV. As interaction factors, the values $f_{p\sigma}$ = 1.267 and $f_{p\pi}$ = 0.525 were used. SCF Molecular orbitals were obtained at the RHF (Restricted Hartree–Fock) and ROHF (Restricted Open-Shell Hartree–Fock) levels for the closed-shell (Ru^{II}) and open-shell (Ru^{III}) ground state species, which correspond to the normal $(t_{2g})^6$ and $(t_{2g})^5$ configurations, respectively. Electronic spectra were generated by single CI excitations in a symmetric active space involving 20 frontier molecular orbitals (10 highest occupied and 10 lowest unoccupied MOs). The nuclear co-ordinates used were obtained from the crystallographic data for the [Ru(bipy)$_2$(sal)] complex. Geometry optimizations were carried out as necessary, using the MM^+ module, a modified MM2 force field[19] within the HyperChem 4.5 program. In this case, a gradient of 1×10^{-5} kcal $Å^{-1}$ mol^{-1} was used as a convergence criterion in a conjugate gradient method. All the calculations were processed on a SGI Indigo^2 R10000 workstation.

Results and discussion

Crystal structure of [Ru(bipy)$_2$(sal)]·4H_2O

The molecular structure of [Ru(bipy)$_2$(sal)] is shown in Fig. 1, and selected bond distances and angles are given in Table 1. The ruthenium(II) ion is chelated by two bipyridine and one salicylate ligand. The Ru–N(1) and Ru–N(4) distances are equivalent, as expected from their symmetric localization; however, the Ru–N(2) bond (2.018 Å) is significantly shorter than Ru–N(3) (2.038 Å). On the other hand, the Ru–O(2) bond distance (2.069 Å) is longer than Ru–O(1) (2.042 Å), indicating that the carboxylate oxygen is more weakly bound than the phenolate group. The bipyridine rings are approximately coplanar, exhibiting a dihedral angle of 5.6°. The ruthenium–salicylate moiety is essentially planar.

There are four molecules of water associated with each ruthenium complex in the crystal. Hydrogen bonds can be detected between the lattice water molecules and the non-coordinated carboxylic oxygen (typical O···O distance = 2.69 Å), as well as between the water molecules themselves (typical O···O distance = 2.86 Å).

Table 1 Selected bond lengths (Å) and angles (°) for [Ru(bipy)$_2$(sal)]·4H_2O

Ru–N(1)	2.042(5)	Ru–O(1)	2.042(4)
Ru–N(2)	2.018(5)	Ru–O(2)	2.069(4)
Ru–N(3)	2.038(5)		
Ru–N(4)	2.047(5)		
N(2)–Ru–N(1)	79.5(2)	N(1)–Ru–O(1)	87.5(2)
N(3)–Ru–N(4)	79.4(2)	N(2)–Ru–O(1)	87.1(2)
		N(3)–Ru–O(2)	86.3(2)
N(2)–Ru–N(3)	96.9(2)	N(4)–Ru–O(2)	88.7(2)
N(2)–Ru–N(4)	97.0(2)	N(1)–Ru–O(2)	94.8(2)
N(3)–Ru–N(1)	99.0(2)	N(4)–Ru–O(1)	94.3(2)
N(1)–Ru–N(4)	176.0(2)	N(2)–Ru–O(2)	173.8(2)
		N(3)–Ru–O(1)	172.8(2)
O(1)–Ru–O(2)	90.2(2)	C(1)–O(1)–Ru	125.6(4)
		C(7)–O(2)–Ru	129.2(4)
C(8)–N(1)–Ru	127.2(4)	C(18)–N(3)–Ru	126.1(5)
C(12)–N(1)–Ru	114.8(4)	C(22)–N(3)–Ru	115.4(4)
C(13)–N(2)–Ru	115.3(4)	C(23)–N(4)–Ru	115.4(4)
C(17)–N(2)–Ru	126.3(4)	C(27)–N(4)–Ru	125.8(5)

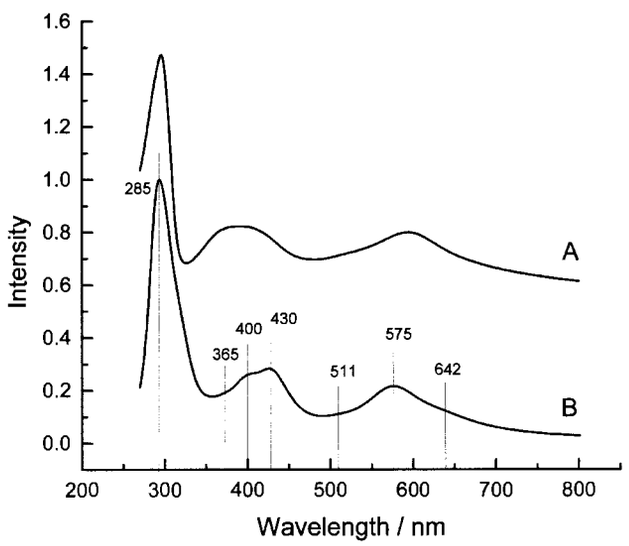

Fig. 2 Electronic spectra of [Ru(bipy)$_2$(sal)]: (A) experimental and (B) ZINDO/S calculated bands and theoretical simulation assuming a half-bandwidth of 2000 cm^{-1} and Lorentzian lines.

Electronic and resonance Raman spectra of [Ru^{II}(bipy)$_2$(sal)]

The electronic spectrum of the [Ru^{II}(bipy)$_2$(sal)] complex consists of three broad, composite bands around 590, 400 and 290 nm, as shown in Fig 2A. The low energy band is rather peculiar, since for ruthenium polypyridine complexes the ruthenium(II)-to-bipy charge-transfer bands are usually observed in the 400–500 nm range. On the other hand, the salicylate ligand is a typical donor species which forms stable complexes with metal ions in relatively high oxidation states. Therefore, low energy ruthenium(II)-to-salicylate charge transfer bands are not expected, as would be the case of complexes with π-acceptor ligands.

In order to elucidate this point, theoretical calculations were carried out using the spectroscopic implementation of the ZINDO semiempirical method, ZINDO/S (see Experimental

Table 2 Electronic spectrum of [Ru(bipy)(sal)]

Experimental		Calculated (ZINDO/S)			
λ/nm	ε/M^{-1} cm^{-1}	λ/nm	Osc. strength	Transition[a] $MO_i \longrightarrow MO_f$	Assignment
290	3.0×10^4	283, 289	0.686, 0.408	80, 81 ⟶ 88	Internal bipy
400[c]	8.1×10^3	365	0.040	85, 87 ⟶ 92; 86 ⟶ 93	LLCT/MLCT[b]
		390, 400	0.094, 0.121	87 ⟶ 92; 86 ⟶ 91	LLCT, MLCT
		430	0.110	86,87 ⟶ 90; 87 ⟶ 91	MLCT/LLCT[b]
590[d]	7.3×10^3	511	0.028	86 ⟶ 89	MLCT
		575	0.245	85, 86 ⟶ 88	MLCT
		642	0.048	86 ⟶ 88; 87 ⟶ 89	MLCT/LLCT[e]

[a] Only the main components of the transition. [b] Predominant character. [c] A broad composite band from 330 to 460 nm. [d] An envelope from 490 to near 800 nm containing at least 3 bands (maximum absorption around 590 nm). [e] MLCT and LLCT with equivalent character.

Table 3 MO Energy order and fractional orbital mixing of [Ru(bipy)$_2$(sal)]

MO	Energy/eV	Ru	bipy	sal
80	−8.893	0.009	0.974	0.017
81	−8.853	0.003	0.991	0.006
82	−8.176	0.012	0.005	0.983
83	−7.872	0.059	0.021	0.920
84	−7.726	0.351[a]	0.125	0.524
85	−7.035	0.615[b]	0.178	0.207
86	−6.684	0.535[c]	0.327	0.138
87 (HOMO)	−6.415	0.285[d]	0.085	0.630
88 (LUMO)	−1.351	0.054	0.939	0.007
89	−1.160	0.092	0.894	0.014
90	−0.671	0.008	0.991	0.001
91	−0.531	0.047	0.948	0.005
92	−0.294	0.023	0.975	0.002
93	−0.242	0.029	0.967	0.004
94	0.434	0.002	0.997	0.001

[a] 0.074 d_{xy} + 0.107 d_{xz} + 0.018 d_{yz} + 0.041 $d_{x^2-y^2}$ + 0.110 d_{z^2} (+4s and 4p). [b] 0.027 d_{xy} + 0.002 d_{xz} + 0.125 d_{yz} + 0.431 $d_{x^2-y^2}$ + 0.028 d_{z^2} (+4s and 4p). [c] 0.066 d_{xy} + 0.176 d_{xz} + 0.055 d_{yz} + 0.088 $d_{x^2-y^2}$ + 0.145 d_{z^2} (+4s and 4p). [d] 0.039 d_{xy} + 0.080 d_{-xz} + 0.042 d_{yz} + 0.009 $d_{x^2-y^2}$ + 0.113 d_{z^2} (+4s and 4p).

and computational section for more details about the calculations). The results from the spectral simulation were surprisingly good, as shown in Fig. 2B and Table 2, supporting the assignment of the visible bands in terms of ruthenium(II)-to-pyridine charge-transfer transitions predicted at 365, 400, 511 and 575 nm, involving two occupied, predominantly d_π metal levels (Table 3) split in a low symmetry field [MO numbers 85 (61.5% Ru) and 86 (53.5% Ru)] and three sets of nearly degenerate π*(bipy) empty levels [MO numbers 88 (LUMO), 89; 90, 91 and 92, 93 (all > 90% bipy)]. Although other bands show a minor LLCT character, the one at 430 nm may be ascribed predominantly to a salicylate-to-bipyridine charge transfer, since it involves primarily the MO 87 (HOMO; 63.0% sal) and the unoccupied MO 90 and 91 (bipy) levels. A low energy transition is expected at 642 nm, involving the occupied MOs 86 (Ru) and 87 (HOMO; sal) and the unoccupied MOs 88 and 89 (essentially bipy), exhibiting balanced ligand-to-ligand and metal-to-ligand charge-transfer characters (MLCT/LLCT). This feature has also been recently observed in other related systems.[21,22] The absorption band at 290 nm (calculated at 285 nm) can be assigned to π ⟶ π* internal transitions in the bipyridine ligand (Table 2). According to the theoretical calculations, these transitions also exhibit a substantial charge-transfer character due to the strong mixing of the ruthenium and bipy π orbitals (see Table 3 for a complete description of the ordering and the fractional mixing of the molecular orbitals).

Typical resonance Raman spectra of [Ru^{II}(bipy)$_2$(sal)] are shown in Fig. 3. In addition to the intensity variations, which followed approximately the absorption profile, the enhanced peaks in the Raman spectra were characteristic of bipyridine

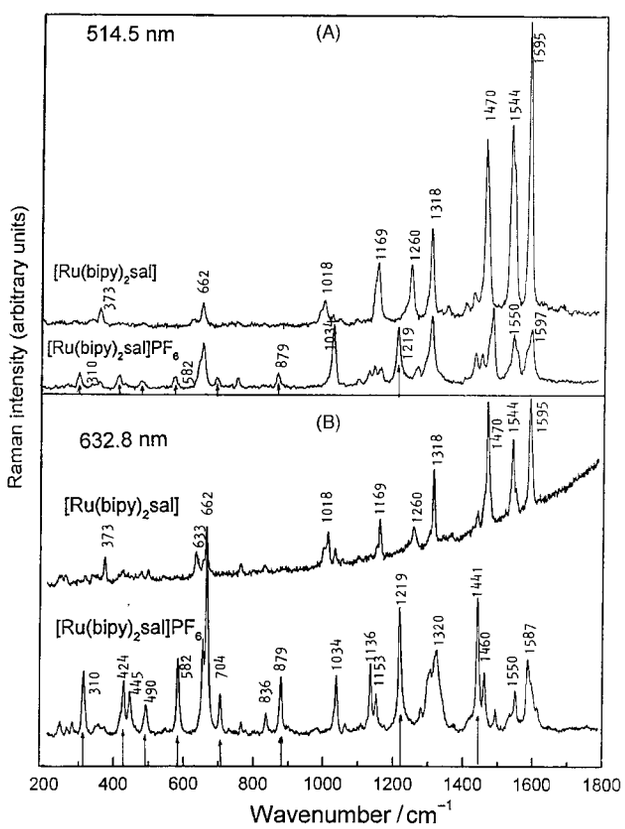

Fig. 3 Typical resonance Raman spectra of [Ru(bipy)$_2$(sal)] and the oxidized product [Ru(bipy)$_2$(sal)]PF_6 obtained at (A) λ_{exc} = 514.5 nm, (B) λ_{exc} = 632.8 nm, using pure solid samples (the salicylate peaks are indicated by an arrow).

vibrational modes, *i.e.* at 1595, 1544, 1470 ($\nu_{CC,CN}$); 1318, 1260 ($\nu_{CC,CN}$ + δ_{CCH}); 1169, 1018 (δ_{CCH} + ν_{CC}); 662 (δ_{CCC} + ν_{RuN}); 373 cm^{-1} (ν_{RuN} + a_{CCC}). The Raman spectra were very similar to those observed for related ruthenium(II)–bipyridine complexes,[13–16,23] reinforcing our assignment of the charge-transfer bands in the visible region.

Electrochemical and spectroelectrochemical behavior

Characterization of the green oxidation product. Typical cyclic voltammograms for the [Ru(bipy)$_2$(sal)] complex are shown in Fig. 4. By starting at −0.1 V and scanning in the direction of more positive potentials, a reversible wave (1) was observed at 0.24 V. Apparently, the position of this wave is unusual for ruthenium-(II)-(III) polypyridine complexes; however it fits the linear correlation between the redox potentials and the Ru^{II}–bipy MLCT wavenumbers previously reported for [Ru(bipy)$_2$L$_2$] complexes,[24] eqn. (1). For E(Ru$^{III/II}$ = 0.24 V, the expected wavenumber for the Ru–bipy MLCT band is 17300 cm^{-1} (575 nm), while the observed one is 16700 cm^{-1} (590 nm).

Table 4 MO Energy order and fractional orbital mixing of $[Ru(bipy)_2(sal)]^+$

MO	Energy/eV	Ru	bipy	sal
80	−11.784	0.002	0.990	0.008
81	−11.708	0.006	0.983	0.011
82	−11.665	0.729[a]	0.077	0.194
83	−11.032	0.015	0.005	0.980
84	−10.892	0.471[b]	0.236	0.293
85	−10.698	0.521[c]	0.185	0.294
86	−10.552	0.019	0.008	0.973
87 (HOMO)	−9.871	0.161[d]	0.079	0.760
88 (LUMO)	−4.352	0.031	0.964	0.005
89	−4.227	0.044	0.951	0.005
90	−3.566	0.004	0.995	0.001
91	−3.513	0.015	0.983	0.002
92	−3.231	0.009	0.990	0.001
93	−3.130	0.009	0.989	0.002
94	−2.474	0.001	0.998	0.001

[a] 0.031 d_{xy} + 0.012 d_{xz} + 0.061 d_{yz} + 0.295 $d_{x^2-y^2}$ + 0.328 d_{z^2} (+4s and 4p). [b] 0.106 d_{xy} + 0.282 d_{xy} + 0.015 d_{yz} + 0.042 $d_{x^2-y^2}$ + 0.023 d_{z^2} (+4s and 4p). [c] 0.068 d_{xy} + 0.020 d_{xz} + 0.164 d_{yz} + 0.190 $d_{x^2-y^2}$ + 0.075 d_{z^2} (+4s and 4p). [d] 0.018 d_{xy} + 0.060 d_{xz} + 0.002 d_{yz} + 0.055 $d_{x^2-y^2}$ + 0.025 d_{z^2} (+4s and 4p).

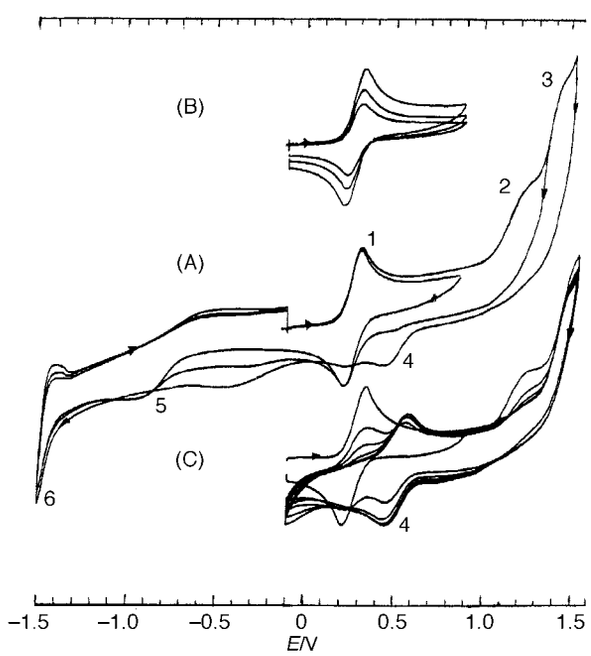

Fig. 4 (A) Cyclic voltammograms of $[Ru(bipy)_2(sal)]$, 1 mmol dm^{-3} in dmf, showing (B) the reversible behavior of the starting complex at 100, 50 and 20 mV s^{-1} and (C) the formation of a new, reversible couple in the reverse scan, after reaching 1.5 V.

$$E\,(\mathrm{MLCT, cm^{-1}}) = 5242\,E\,(\mathrm{Ru^{III/II}, V\ \textit{vs.}\ NHE}) + 16130 \quad (1)$$

Therefore, the $E(Ru^{III/II})$ value is consistent with the red shift of the Ru–bipy MLCT band, reflecting the influence of the donor properties of the salicylate ligand. The presence of a donor ligand should stabilize the higher oxidation state, decreasing $E°$, but in a limiting case the donor ligand can also be oxidized, competing with the metal center. By working under equivalent conditions, however, the first oxidation peak in the electrochemistry of free salicylate appeared at relatively high potentials (0.9 V), ruling out this hypothesis.

Spectroelectrochemical measurements associated with this wave in the complex exhibited a reversible behavior, as shown in Fig. 5A. The oxidized product displayed a deep green color, and was stable enough to be isolated as a solid (see Experimental section). The spectrum of the oxidized product consisted of two absorption bands in the visible region, at 700 and 420 nm, departing from the typical spectra of the ruthenium-(II) or -(III)

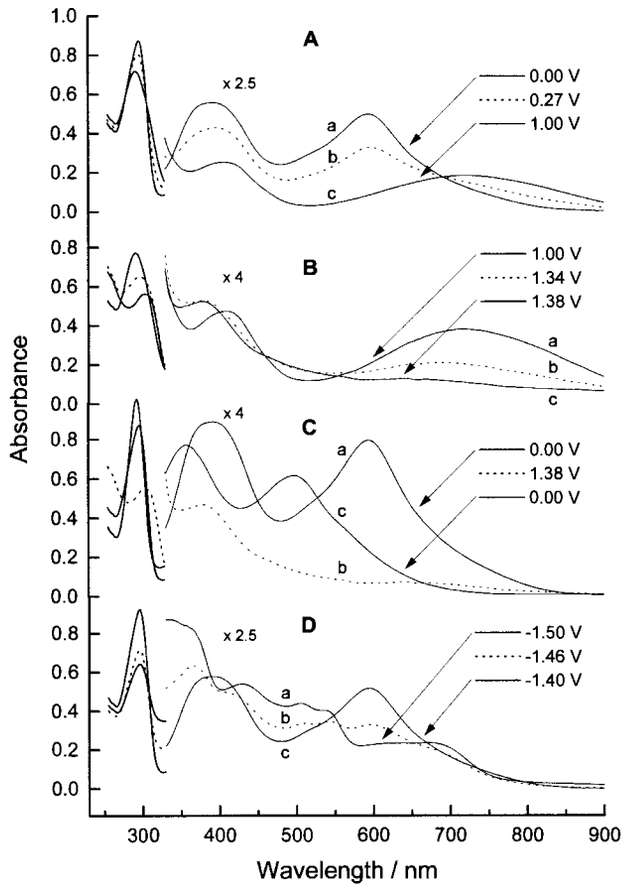

Fig. 5 Spectroelectrochemistry of the [Ru(bipy)(sal)] complex in dmf solutions, showing (A) the reversible behavior of the starting complex, (B) the decay of the visible absorption bands accompanying the oxidation processes at 1.38 V, (C) the formation of a new species after returning the potential from 1.38 to 0 V, and (D) the spectral changes associated with the reduction of the bipy ligand, at −1.5 V.

polypyridine complexes, or from any kind of spectroelectrochemical correlation reported before.

Theoretical calculations for the $[Ru(bipy)_2(sal)]^+$ complex (Table 4), based on the ZINDO/S method, revealed that: among the six highest occupied levels, one is mainly Ru (d_π) [MO 82 (72.9% Ru)], two exhibit extensive Ru–bipy–salicylate mixing [*e.g.* MOs 84 (47.1% Ru + 23.6% bipy + 29.3% sal) and 85 (52.1% Ru + 18.5% bipy + 29.4% sal)] and three exhibit predominantly a salicylate character [MOs 83 (98.0% sal), 86 (97.3% sal) and 87 (76.0% sal)]. The fact that the frontier occupied orbital (HOMO; number 87) is made up of, in its majority, salicylate ligand and only 16% of Ru^{III} (d_π) suggests a description of the oxidized complex as $[Ru^{II}(bipy)_2(sal^+)]^+$ better than $[Ru^{III}(bipy)_2(sal)]^+$. On the other hand, the lowest unoccupied levels [MOs 88 (LUMO), 90 and 91)] are essentially bipy (p_π*) (>95% bipy). The spectral simulations were not as good as in the case of the starting complex, however a series of transitions were located in the 350–700 nm range, from the HOMO 83–87 (donor) levels to the LUMO 88–91 (acceptor) levels. Considering the nature of the HOMO and LUMO levels involved in the electronic transitions, it should be noted that there is a strong electronic mixing of the ruthenium–bipy–salicylate π orbitals in the HOMO levels. The electronic transitions exhibit pronounced (salicylate + bipy) ligand-to-metal charge transfer character, as well as (salicylate-to-bipy) ligand-to-ligand charge transfer, as observed in many quinonoid complexes.[2–6,21,22] As an indication of strong electronic coupling, EPR measurements for the green solid at room temperature, as well as at 220 K, exhibited no evidence of the multiplet signals characteristic of aromatic semiquinone radicals, or of the typical ruthenium(III) signals.

Resonance Raman spectra for the green oxidized species revealed a simultaneous enhancement of the bipyridine and salicylate vibrations, as shown in Fig. 3. The bipyridine peaks at 1587, 1550, 1460, 1320, 1153, 1136, 1034, 662, and 370 cm^{-1} (the 370 cm^{-1} band occurs at low intensity) practically coincide with those observed for the reduced species. The salicylate peaks were identified based on a recent study on the resonance Raman spectra of the ligand, at 1441 ($\nu_{COO} + \nu_{14}$), 1219 (ν_{C-O^-}), 879 ($\nu_{C-COO^-} + \nu_{C-O^-}$), 704 ($\nu_{11}$), 582 ($\varphi_{CCC} + \rho_{COO^-}$), 490 ($\varphi_{CCC} + \delta_{C-O^-}$) and 424 cm^{-1} (ν_{16}) where the frequency notations refer to Wilsons numbering for benzene vibrational modes.[25] The peak at 310 cm^{-1} was ascribed to the Ru–O vibrational mode based on its strong enhancement, and on its absence in the spectra of the bipyridine and salicylate ligands. The enhancement of the bipyridine and salicylate ligand vibrations confirms the hypothesis of a strong mixing of the ligand orbitals in the oxidized complex, as is the case of the ruthenium polypyridine complexes with quinonoid and related ligands.[2–6]

Electrochemical oxidation of the green species. Further oxidation of the green $[Ru(bipy)_2(sal)]^+$ complex, generated at 0.24 V, was evidenced by two successive, irreversible waves at 1.2 and 1.4 V (waves 2 and 3 in Fig. 4A). The corresponding spectroelectrochemical changes (Fig. 5B) cannot be discriminated due to the close proximity of the redox waves and to their irreversible nature. The oxidation wave at 1.2 V can be ascribed to the monoelectronic oxidation of salicylate ligand, based on the electrochemical behavior of the sodium salicylate species, and on the consideration that by reversing the potential scan at this point the voltammogram of the starting complex is regenerated (see Fig. 4A). Therefore, the co-ordinated ligand remains intact up to this point. At 1.4 V, however, the oxidation process leads to an irreversible chemical change, generating a new species that exhibits, in the reverse scan, a reversible wave (4) at 0.55 V, as shown in the cyclic voltammograms of Fig. 4C. The isolation of this species has not been successful up to the present time; however, the spectroelectrochemical results shown in Fig. 5C-c resemble those associated with typical ruthenium(II)–polypyridine complexes. Therefore, one can propose that the electrochemical process at 1.2 V involves the oxidation of the salicylate ligand to the semiquinone form, which is further oxidized at 1.4 V, generating a very reactive electrophilic species. In the presence of water molecules or OH^- ions, hydroxylation proceeds very fast,[1] yielding the 4-hydroxysalicylate semiquinone complex as the most probable species, as shown in Scheme 1.

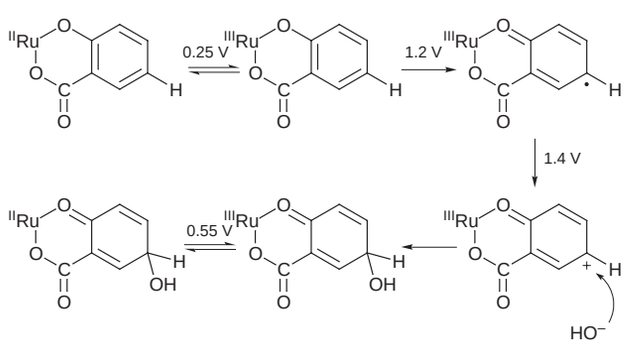

Scheme 1

The ZINDO/S spectral simulations for this complex reproduced the absorption profile centered around 500 nm, in Fig. 5C-c, showing, in addition, a series of ruthenium(II)-to-bipy d_π–p_π charge-transfer transitions at 590 (weak), 500 (strong), 440 (weak), 400 (weak) and 380 nm (weak). The location of the main MLCT band at 500 nm is consistent with the expected value (520 nm, for $E^\circ = 0.55$ V) based on the reported spectroscopic–electrochemical correlation for $[Ru(bipy)_2L_2]$ complexes.[24]

It should be noted that, according to the cyclic voltammograms (Fig. 4), the expected dimerization of the radical species generated at 1.2 V (wave 2) does not compete with the oxidation process at 1.4 V (wave 3). In fact, the dimerization process does not require any additional electron transfer, and cannot be ascribed to the oxidation wave observed at 1.4 V. This process is actually responsible for the formation of the product absorbing at 500 nm. According to ZINDO/S calculations, the spectrum of the dimeric product would be very similar to that of the $[Ru(bipy)_2(sal)]$ complex, departing from the observed results shown in Fig. 5C(a,c).

Electrochemical reduction of the $[Ru(bipy)_2(sal)]$complex. An irreversible wave (5) was observed at −1.0 V, by scanning the potential in the direction of negative potentials (Fig. 4). The intensity and shape of this wave vary with the potential employed in the reverse scan (see Fig. 4). Since there were no detectable changes in the electronic spectra of the complex, the most plausible assignment would be the reduction of the water molecules, as well as of the protons released from the hydroxylation process. In contrast, the reduction of the bipyridine ligands can be detected at −1.5 V (wave 6, in Fig. 4), from the decay of the absorption band in the UV region, and the dramatic changes in the absorption bands in the visible region (Fig. 5D).

Conclusion

Salicylic acid forms a stable mixed-ligand complex with bis(bipyridine)ruthenium(II), displaying low energy electronic bands mainly associated with ruthenium-to-bipy charge-transfer transitions. Oxidation proceeds reversibly at 0.24 V generating an unusual green species involving a strong ruthenium–salicylate electronic delocalization. Further oxidation of the green complex leads to hydroxylation of the salicylate semiquinone ligand in the complex.

Acknowledgements

The support from FAPESP (Fundação de Amparo à Pesquisa do Estado de São Paulo), CNPq (Conselho Nacional de Desenvoluimento Cientifico e Tecnológico) and PADCT (Programa de Apoio ao Desenvoluimento Cientifico e Tecnológico) is gratefully acknowledged. We thank the Laboratório de Espectroscopia Molecular (Instituto de Química, Universidade de São Paulo) for the use of Raman equipment. We would also like to thank Dr Ana M. C. Ferreira (Instituto de Química, Universidade de São Paulo) for her assistance in EPR experiments.

References

1 B. Kalyanaraman, S. Ramanujam, R. J. Singh, J. Joseph and J. B. Feix, *J. Am. Chem. Soc.*, 1993, **115**, 4007.
2 C. G. Pierpont and C. W. Lange, *Prog. Inorg. Chem.*, 1994, **41**, 331.
3 R. A. Metcalfe and A. B. P. Lever, *Inorg. Chem.*, 1997, **36**, 4762.
4 F. Hartl, T. L. Snoeck, D. J. Stufkens and A. B. P. Lever, *Inorg. Chem.*, 1995, **34**, 3887.
5 H. Masui, A. B. P. Lever and E. S. Dodsworth, *Inorg. Chem.*, 1993, **32**, 258.
6 H. Masui, A. B. P. Lever and P. R. Auburn, *Inorg. Chem.*, 1991, **30**, 2402.
7 B. P. Sullivan, D. J. Salmon and T. J. Meyer, *Inorg. Chem.*, 1978, **17**, 3334.
8 CAD4-EXPRESS, version 5.1, Delft Instruments X-Ray Diffraction, Delft, 1992.
9 L. H. Straver and A. J. Schierbeek, MOLEN Structure Determination System, Enraf-Nonius Corp., Delft, 1994.
10 G. M. Sheldrick, SHELXS 86, in *Crystallographic Computing 3*, eds. G. M. Sheldrick, C. Kruger and R. Goddard, Oxford University Press, Oxford, 1985, p. 175.
11 G. M. Sheldrick, SHELXL 93, in *Crystallographic Computing 6*, eds. H. D. Flack, L. Parkanyi and K. Simons, Oxford University Press, Oxford, 1993, p. 111.
12 B. Kratochvil, E. Lorah and C. Garber, *Anal. Chem.*, 1969, **41**, 1793.

13 H. E. Toma and C. Cipriano, *J. Electroanal. Chem.*, *Interfacial Electrochem.*, 1989, **263**, 313.
14 V. R. L. Constantino, L. F. C. Oliveira, P. S. Santos and H. E. Toma, *Transition Met. Chem.*, 1994, **19**, 103.
15 V. R. L. Constantino, H. E. Toma, L. F. C. Oliveira and P. S. Santos, *J. Raman Spectrosc.*, 1992, **23**, 629.
16 T. E. Chavez-Gil, D. L. A. de Faria and H. E. Toma, *Vibrational Spectrosc.*, 1998, **16**, 89.
17 M. C. Zerner, G. H. Loew, R. F. Kirchner and U. T. Mueller-Westerhoff, *J. Am. Chem. Soc.*, 1980, **102**, 589.
18 ZINDO, A comprehensive semiempirical SCF/CI package, M. C. Zerner and co-workers, University of Florida, Gainesville, FL, 1995.
19 N. L. Allinger, *J. Am. Chem. Soc.*, 1977, **99**, 8127; HyperChem 4.5, Hypercube, Inc., Gainesville, FL, 1995.
20 C. K. Johnson, ORTEP II, Report ORNL-5138, Oak Ridge. National Laboratory, Oak Ridge, TN, 1976.
21 M. D. Ward, *Inorg. Chem.*, 1996, **35**, 1712.
22 W. Paw, W. B. Connick and R. Eisenberg, *Inorg. Chem.*, 1998, **37**, 3919.
23 P. K. Mallick, G. D. Danzer, D. P. Strommen and J. R. Kincaid, *J. Phys. Chem.*, 1988, **92**, 5628.
24 B. K. Ghosh and A. Chakravorty, *Coord. Chem. Rev.*, 1989, **95**, 239.
25 B. Humbert, M. Alnot and F. Quiles, *Spectrochim. Acta*, *Part A*, 1998, **54**, 465.

Paper 9/02219H